Micro-scale Auxetic Hierarchical Mechanical Metamaterials for Shape Morphing

*K. K. Dudek, J. A. Iglesias Martínez, G. Ulliac, M. Kadic**

K. K. Dudek, J. A. Iglesias Martínez, G. Ulliac, M. Kadic
Institut FEMTO-ST, CNRS, Université Bourgogne Franche-Comté, Besançon 25030, France
K. K. Dudek
Institute of Physics, University of Zielona Gora, ul. Szafrana 4a, 65-069 Zielona Gora, Poland
Email Address: muamer.kadic@femto-st.fr

Keywords: *mechanical metamaterials, hierarchical metamaterials, auxetic, shape morphing*

Shape morphing and the possibility of having control over mechanical properties via designed deformations have attracted a lot of attention in the materials community and led to a variety of applications with an emphasis on the space industry. However, current materials normally do not allow to have a full control over the deformation pattern and often fail to replicate such behavior at low scales which is essential in flexible electronics. Thus, in this paper, we propose novel 2D and 3D microscopic hierarchical mechanical metamaterials using mutually-competing substructures within the system that are capable of exhibiting a broad range of the highly unusual auxetic behavior. Using experiments (3D microprinted polymers) supported by computer simulations, we show that such ability can be controlled through geometric design parameters. We finally demonstrate that the considered structure can form a composite capable of shape morphing allowing it to deform to a predefined shape.

1 Introduction

Shape morphing [1, 2, 3, 4, 5, 6, 7, 8], utilising the topological or space time properties [9, 10, 11] and the ability to control mechanical properties [12] of functional materials [13, 14, 15, 16, 17, 18, 19, 20, 21, 22, 23] remain some of the main challenges in materials science. At the same time, the possibility of constructing materials possessing such properties is in high demand as it may lead to the design of structures superior to currently known biomedical and other devices used in various industries. In addition, the task of designing and manufacturing such materials becomes even more difficult at small scales such as the microscale that are crucial from the point of view of many new types of applications, e.g. flexible electronics [24, 25] and specialized medical equipment [26, 27]. However, despite the level of difficulty, over the years, it has been possible to note an emergence of promising directions of studies that address the possibility of observing these effects. In fact, one of the most interesting directions of studies related to this topic are mechanical metamaterials [28, 29, 30, 3, 31, 32], i.e. structures that can exhibit counterintuitive mechanical behavior based primarily on their design. Mechanical metamaterials are known for their ability to exhibit counterintuitive mechanical properties such as auxetic behavior [33, 34, 35, 36, 37, 38, 39, 40], negative stiffness [2, 41] and negative compressibility [42, 43] that are essential in many industries. However, in a vast majority of cases, standard mechanical metamaterial proved insufficient while searching for structures capable of exhibiting versatile deformation patterns. This in turn led to intensive studies devoted to hierarchical mechanical metamaterials [44, 45, 46], i.e. structures composed of elements having their own geometry that normally can deform irrespective of the rest of the system.

Despite the large popularity of hierarchical mechanical metamaterials, it is a relatively new thread in the field of mechanical metamaterials. It seems that some of the first studies devoted to this topic were published by Gatt *et al.* [45] and Cho *et al.* [46] where the famous hierarchical rotating square system was proposed. In the following years, it was demonstrated [45, 46, 47, 48, 49] that this structure can exhibit tunable auxetic behavior where the extent of auxeticity depends on the relative rate of the deformation of hierarchical levels constituting the system. Recently, it was also reported that the design of the hierarchical square system can be modified in order to change its characteristic [50, 51, 4, 52, 53]. Similar studies based primarily on the extent of the observed auxeticity were also conducted for structures based on rotating rectangles [54] as well as re-entrant and other honeycombs [54, 55, 56, 57, 58].

Even though the concept of hierarchical mechanical metamaterials proved to be very popular and resulted in numerous publications, it is possible to note that the hierarchical structures proposed up to

date normally share several limitations. First, most of the known hierarchical mechanical metamaterials are designed in a way where their different hierarchical levels correspond either to the same deformation mechanism or to structures having very similar Poisson's ratio. Hence, the possible range of the resultant auxetic behavior is relatively small and may prove to be insufficient in the case of applications where functional materials must significantly change their mechanical response. Another limitation of the already reported hierarchical metamaterials is the fact that in a vast majority of cases, their ability to exhibit the tunable mechanical behavior was only demonstrated for macroscopic prototypes. On the other hand, there are numerous types of applications (e.g. biomedical devices and flexible electronics) where similar materials with the ability to exhibit programmable auxetic behavior would be of great importance at a much lower scale with the emphasis on the mico-scale. Finally, almost all of the reported hierarchical metamaterials are two-dimensional systems which lowers their applicability. Thus, the possibility of designing three-dimensional hierarchical metamaterials [59, 60, 61] capable of exhibiting programmable control over mechanical properties in multiple directions would be of great significance.

We propose novel 2D and 3D micro-scale hierarchical mechanical metamaterials. In addition, by means of experiments supported by Finite Element Method (FEM) simulations, it is demonstrated that the considered structure is capable of exhibiting controllable auxetic behavior upon changing the thickness of hinges connecting its structural elements. In this regard, thanks to the very novel design resulting in the mutually-competing substructures being present within the system, it is showcased that the analyzed model may exhibit a very broad range of the auxetic behavior which in turn increases its applicability and the appeal for researchers in the field of materials science. Finally, it is shown that the analyzed mechanical metamaterial may exhibit a predefined shape morphing. In other words, it is shown that thanks to its hierarchical design, the considered mechanical metamaterial can change its shape in order to match the shape of another object upon being subjected to an external stimulus.

2 Results and discussion

In this work, novel 2D and 3D hierarchical mechanical metamaterials are designed in order to assess their ability to exhibit a wide range of auxetic behavior as well as shape morphing. As shown in **Fig. 1(a)**, the 2D version of the considered system is a two-level hierarchical structure. However, unlike in the case of a vast majority of the already known hierarchical mechanical metamaterials, the deformation mechanisms corresponding to each of the hierarchical levels of the system are very different. More specifically, as shown in **Fig. 1(b)**, the structure selected to form level 0 of the system corresponds to the non-auxetic rotating triangles structure with its unit-cell having a shape of a rectangle. This geometry was first proposed by Milton *et al.* [13] where it was used in order to construct mechanical expanders capable of significantly changing their dimensions during the deformation process. A few years later, Dudek *et al.* [62] demonstrated that this specific mechanical metamaterial never exhibits auxetic behavior in the axial directions, and instead it can be characterized by the negative linear compressibility irrespective of the geometric parameters used to define it. On the other hand, the deformation mechanism associated with level 1 of the structure corresponds to the rotating square [63] / rectangle [64] system proposed initially by Grima *et al.* with the rotating square-like geometries being famous for their ability to exhibit auxetic behavior. In view of this, the deformation of the hierarchical system considered in this work corresponds to the interplay between the two hierarchical levels associated with a positive (level 0) and negative (level 1) Poisson's ratio respectively (this interplay is referred to as mutually-competing substructures). Thus, depending on the extent of the mechanical deformation of the two hierarchical levels, it is expected that the Poisson's ratio of the entire structure can be significantly modified. At this point, it should be mentioned that even though in this work a specific configuration of rotating triangles is considered, in the literature, there are also other types of triangle-based geometries [65, 66, 67, 68] that in general may exhibit other forms of the unusual mechanical behavior.

In terms of the geometry, the two-dimensional analog of the analyzed structure corresponds to the two-

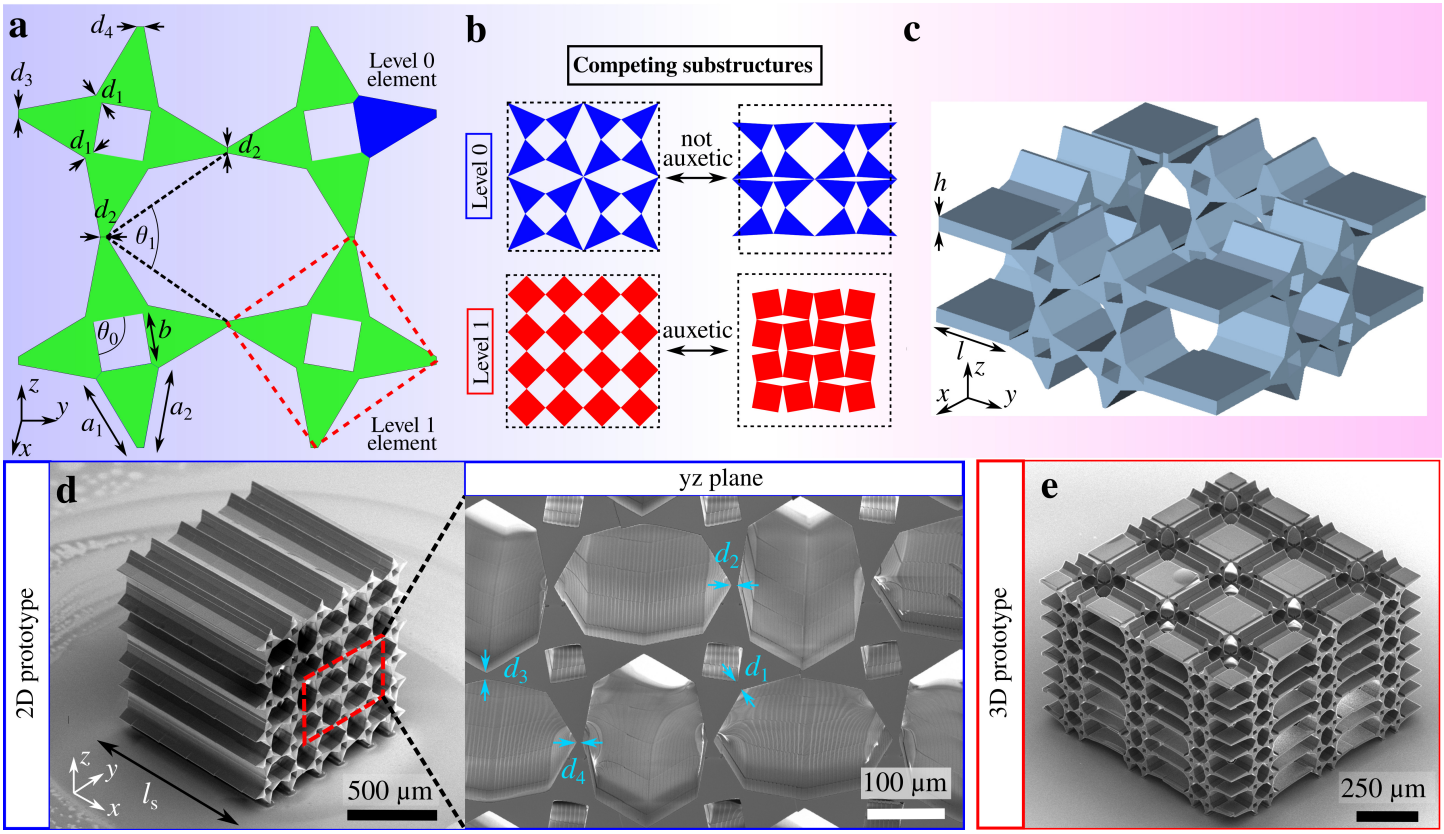

Figure 1: The design of 2D and 3D hierarchical structure considered in this work. **a)** A cross-section of the unit-cell of the considered model having level 1 structural elements composed of 4 (2×2) level 0 units. **b)** Conceptual deformation of substructures corresponding to level 0 and level 1 of the analyzed system. **c)** The unit-cell of the 3D model considered in this study. **d)** SEM (Scanning Electron Microscopy) picture of the quasi-2D experimental prototype composed of 3×3×3 unit-cells. **e)** SEM picture of the 3D experimental prototype consisting of 3×3×4 unit-cells.

level hierarchical structure where level 0 is composed of structural elements closely resembling isosceles triangles (see **Fig.1(a)**). On the other hand, level 1 structural elements correspond to rectangle-like motifs that for the specific case of $\theta_0 = 90°$ assume a shape of a square. In the case of the provided example (see **Fig.1(a)**), level 1 structural elements are composed of 2×2 level 0 units. However, in general, within the frame of the considered model, level 1 blocks can be constructed by means of a different number of $2N_x \times 2N_y$ level 0 elements (e.g. 4×4) assuming that they form a rectangle-like lattice and are connected to each other as shown in **Fig.1**. Furthermore, one should note that even though the structure portrayed in **Fig. 1(d)** is being referred to as being two-dimensional, in reality, it has a non-zero out-of-plane thickness that corresponds to the variable l_s. In addition, it should be emphasized that the unit-cell of the 3D version of the considered hierarchical mechanical metamaterial is very similar to its 2D equivalent. As shown in **Fig. 1(c)**, walls of the unit-cell of the 3D system are almost identical to the 2D unit-cell with the addition of solid blocks having dimensions $l \times l \times h$ that help to connect adjacent walls.

In this work, to analyze the mechanical behavior of the considered hierarchical structure, the entire system is being compressed along the z-axis (see **Fig. 1**) with its bottommost elements being fixed in space. Furthermore, to assess its ability to exhibit a versatile mechanical behavior with a broad range of the exhibited Poisson's ratio, several different structures are investigated with each of them corresponding to a different thickness of hinges connecting structural elements.

2.1 2D hierarchical metamaterials - control over mechanical properties

In order to assess the ability of the considered model to exhibit a tunable Poisson's ratio, three different quasi-2D hierarchical structures (see **Fig. 2**) are considered with the main difference between them being the thickness of hinges connecting level 0 and level 1 elements.

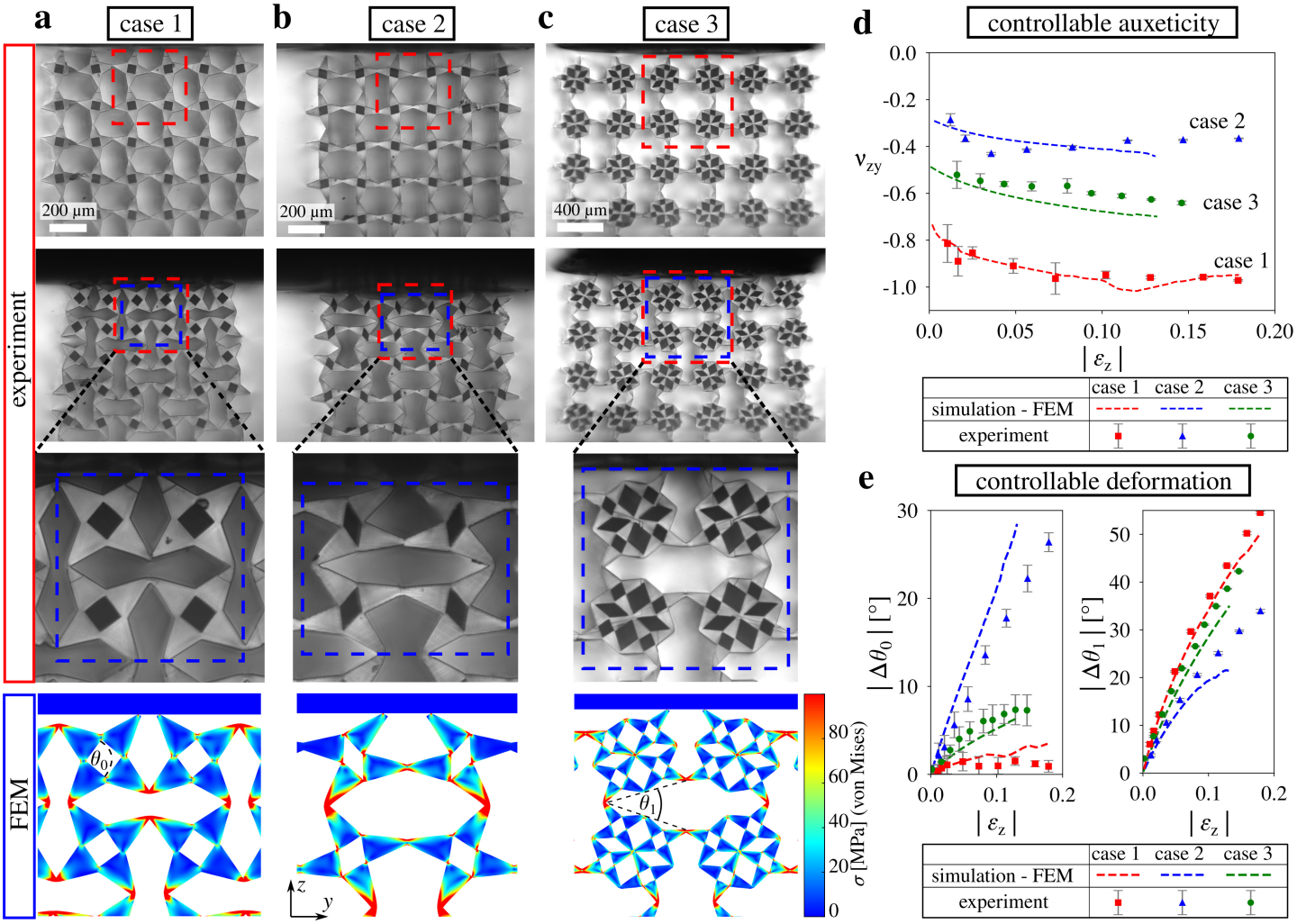

Figure 2: Deformation of the three examples of 2D systems considered in this work that correspond to different thicknesses of hinges. **a)** The first of the analyzed structures (case 1) where for the predeformed structure $\theta_0 = 90°$, $\theta_1 = 70°$, $d_1 \approx 9.3\,\mu$m, $d_2 \approx 6.1\,\mu$m. **b)** Case 2 with the initial parameters defined as $\theta_0 = 100°$, $\theta_1 = 70°$, $d_1 \approx 2.7\,\mu$m, $d_2 \approx 10.0\,\mu$m. **c)** Case 3 where for the predeformed system $\theta_0 = 100°$, $\theta_1 = 70°$, $d_1 \approx 2.6\,\mu$m, $d_2 = 9.6\,\mu$m. **d)** Poisson's ratio measured for the compression along the z-axis calculated for the central topmost unit-cell. **e)** FEA results corresponding to the variation in the θ_0 and θ_1 angles throughout the deformation process. For all structures, $l_s \approx 1200\ \mu$m. Mechanical metamaterials presented on panels a-b) and c) are composed of $3 \times 3 \times 3$ and $3 \times 3 \times 2$ unit-cells respectively. The remaining geometric parameters used for structures shown on panels a-c) were set to be the following: a) $a_1 \approx 77\,\mu$m, $a_2 \approx 78\,\mu$m, $b \approx 48\,\mu$m, $d_3 \approx 6.3\,\mu$m, $d_4 \approx 6.4\,\mu$m, b) $a_1 \approx 79\,\mu$m, $a_2 \approx 81\,\mu$m, $b \approx 48\,\mu$m, $d_3 \approx 12.7\,\mu$m, $d_4 \approx 10.4\,\mu$m and c) $a_1 \approx 77\,\mu$m, $a_2 \approx 79\,\mu$m, $b \approx 47\,\mu$m, $d_3 \approx 14.3\,\mu$m, $d_4 \approx 10.2\,\mu$m. For all mechanical metamaterials portrayed on panels a-c), the red and blue dashed lines correspond to the outline of the initial and deformed unit-cell respectively. All of the experimental pictures shown on panels a-c) were taken by means of the optical camera. Finally, the surface stress presented graphically for the FEA results on panels a-c) corresponds to the von Mises stress model implemented in the COMSOL Multiphysics software.

As shown in **Fig. 2(a)**, the first of the analyzed structures (case 1) corresponds to the hierarchical system where level 1 building blocks assume a shape of a square since $\theta_0 = 90°$. Based on the pictures taken during the experiment, one can note that during the deformation process corresponding to the compression along the z-axis (see **Supplementary Video 1**), the considered part of the structure, i.e.

the central topmost unit-cell, acts as a typical rotating square system. In other words, level 1 structural blocks retain their shape throughout the deformation and rotate with respect to each other which leads to a change in the angle θ_1. As presented in **Fig. 2(d)**, this deformation mechanism results in the highly negative and almost isotropic Poisson's ratio close to -1, i.e. the extent of auxeticity characteristic for the rotating square system. The specific behavior of the structure referred to in this work as case 1 stems from the fact that hinges connecting level 0 elements are thicker than hinges connecting level 1 blocks ($d_1 \approx 9.3\,\mu$m, $d_2 \approx 6.1\,\mu$m). At the same time, all hinges are thin enough so that all of the unit-cells deform primarily through hinging between their structural elements. As a result, it is much easier for the level 1 blocks to rotate with respect to each other than is the case for level 0 elements where the resistance to the rotational motion is significantly larger. Hence, during the deformation process, θ_1 changes to a large extent while θ_0 approximately retains its value (see **Fig. 2(e)**). At this point, it should be also noted that even though the initial configuration of the system allows for a very large extent of the mechanical deformation, it does not correspond to the fully-open configuration, where $\theta_0 = 90°$ and $\theta_1 = 90°$. This stems from the fact that for such system, it would be difficult to predict the direction of rotation of structural elements since it would depend on the polymer's composition and printing imperfections (see **Supplementary Information**).

According to **Fig. 2(b)**, the hierarchical structure referred to as case 2 exhibits a very different behavior than was observed for case 1. More specifically, during the deformation process (see **Supplementary Video 2**), level 1 blocks having a rectangular shape become significantly flattened in one dimension with the orthogonal dimension being slightly increased (i.e. level 1 blocks exhibit the negative linear compressibility behavior characteristic for the non-auxetic rotating triangle system). Furthermore, the change in the shape of the level 1 blocks is accompanied by the mutual rotation of level 0 elements to a significant extent (see **Fig.2(e)**). As shown in **Fig. 2(d)**, this change in the behavior of the hierarchical structure significantly changes the Poisson's ratio that could be observed for the system referred to as case 1. In fact, the Poisson's ratio assumes much less negative values throughout the entire deformation process that reach the level of -0.38 for the experiment. This drastic change in the behavior of the analyzed system originates from the fact that hinges connecting level 0 elements are significantly thinner than hinges corresponding to level 1 of the system ($d_1 \approx 2.7\,\mu$m, $d_2 \approx 10.0\,\mu$m). As a result, despite a large number of hinges associated with level 0 of the system (16 within the unit-cell), the overall resistance of level 0 elements to the rotational motion is not much different than in the case of level 1. Thus, both hierarchical levels could deform to a significant extent which process is reflected by a large concurrent change in angles θ_0 and θ_1 (see **Fig.2(e)**). At this point, it should also be noted that for cases 1 and 2, a part of the bottommost row of unit-cells is not captured on the provided pictures. This stems from the fact that the lenses used in the experiment (see Methods section) were selected in a way ensuring a high quality of this part of the picture that was taken into account while assessing mechanical properties of the system.

The last of the analyzed 2D structures is referred to as case 3 (see **Fig.2(c)**) and corresponds to a very similar system to the one referred to as case 2. In fact, all of the initial angles, as well as thicknesses of hinges, are almost the same in terms of the aspect ratio for both structures. The only significant difference between them corresponds to the number of level 0 elements constituting level 1 blocks, i.e. for case 3, level 1 blocks consist of 16 level 0 elements instead of 4. As shown in **Fig.2(c)**, this small difference in the design of the structure results in a very different behavior of the hierarchical system during the deformation process (see **Supplementary Video 3**). More specifically, level 1 blocks do not get visibly flattened with respect to the initial configuration as was the case for case 2. Instead, they approximately retain their shape throughout the entire deformation process. According to **Fig. 2(d)**, the change in the number of level 0 units also significantly affects mechanical properties of the system resulting in the greater extent of the auxeticity. This change in the behavior between case 2 and case 3 can be explained upon having a closer look at the number of hinges present within the system. More specifically, upon increasing the number of level 0 units constituting level 1 blocks, the number of hinges connecting level 0 elements is also significantly increased. At the same time, the number of hinges connecting level 1 blocks

remains the same. Thus, upon comparing cases 2 and 3, it is much more difficult to rotate level 0 elements corresponding to case 3. As a result, the deformation of this structure corresponds primarily to the change in the value of θ_1 as opposed to the variation in θ_0 (see **Fig.2(e)**).

At this point, it is also worth noting that all of the structures considered in this study deform primarily through the rotation of their structural elements and not their flexing. More specifically, as shown in Fig. 2, according to the von Mises stress distribution corresponding to the FEA simulations, the main accumulation of the stress can be observed in the vicinity of hinges connecting level 1 blocks. On the other hand, in the remaining parts of the structure, it assumes much lower values not exceeding 50 MPa. Since Young's modulus of the polymer used to manufacture the samples is equal to 4GPa (see Methods section), this means that the local stresses do not result in the change of the shape of structural elements. Instead, as shown on the provided pictures, structural elements approximately retain their shape throughout the entire deformation process. Furthermore, it should be noted that even though in this work we focus on the longitudinal compression of the analyzed structures, in general, one can also compress them from other directions including the transverse direction. As shown in the **Supplementary Information**, the compression of the considered systems in the transverse direction may affect their mechanical properties. Nevertheless, not all of them are affected by a change in the direction of compression to the same extent. More specifically, the behavior of the case 1 system seems to be only marginally affected by the direction of compression. On the other hand, especially at low strains, the Poisson's ratio corresponding to the case 2 structure is visibly altered.

2.2 3D hierarchical system

As mentioned in the Introduction, almost all of the known hierarchical mechanical metamaterials are two-dimensional structures which limits their applicability as they can only exhibit their properties in one plane. Thus, it is essential to identify structures that could also exhibit a controllable mechanical response in the case of 3D systems. In fact, one of the first such structures is the hierarchical metamaterial proposed in this work as its ability to exhibit a very broad range of the auxetic behavior is not limited to 2D structures and can be conveniently extended to 3D models. To demonstrate it, we selected two very similar structures referred to as type A and type B. These structures have unit-cells defined as shown in **Fig.1(c)**. In addition, the aspect ratios of hinges and other geometric dimensions corresponding to type A and type B mechanical metamaterials are the same as in the case of the quasi-2D structures named case 1 and case 2 respectively. Hence, based on the already generated results, one should expect the type A structure to be able to exhibit a more auxetic behavior than the type B system. It should be also noted that type A and type B structures look almost identical with the main difference between them being the thickness of hinges. Thus, as an example, a picture of the type A system is shown in Fig. 3(b).

As shown in **Fig. 3(a-b)**, it is indeed possible to construct the microscopic 3D equivalent of the quasi-2D models considered in this work. In addition, upon designing the system composed of unit-cells having the same thickness of hinges as the 2D structure called case 1, it is possible to observe a very strong auxetic response similarly to what was observed for its 2D counterpart (see **Fig.3(a)** and **Supplementary Video 4**). Of course, the extent of the auxeticity in the xz and zy planes is smaller than for the 2D structure and for selected parameters, it maintains the value in the vicinity of -0.4 throughout the entire deformation process (see **Fig.3(c)**). This change in the magnitude of the Poisson's ratio originates from the presence of additional blocks that increase the lateral dimension of the unit-cell in comparison to the case 1 2D structure. Furthermore, upon comparing results corresponding to type A and type B, one can note that in the latter case, the Poisson's ratio assumes significantly less negative values. This in turn is an indication of a possibility to achieve a tunable auxetic behavior similarly to what was the case for 2D systems. It should be also emphasized that the range of negative Poisson's ratio for 3D systems could be further increased if faces of 3D unit-cells were composed of several adjacent structural motifs similar to the geometry presented in **Fig.1**(a). Nevertheless, at the microscale, it would also result in

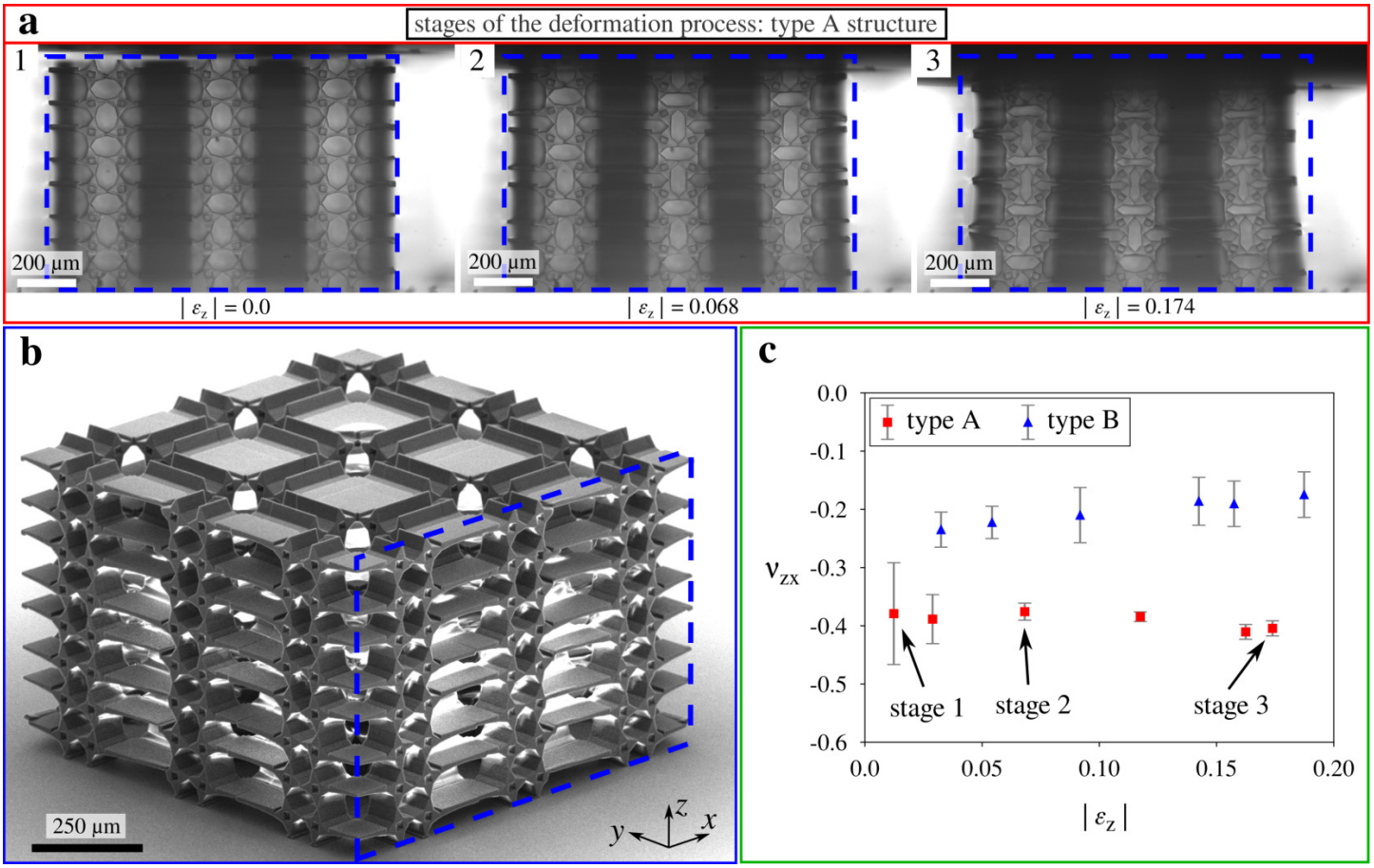

Figure 3: The behavior of the type A and type B 3D hierarchical structures composed of $3 \times 3 \times 4$ and $3 \times 3 \times 3$ unit-cells respectively. Both hierarchical models are subjected to the compression along the z-axis. **a)** Three different stages of the deformation process corresponding to the type A system. Provided pictures were captured by means of the optical camera and portrayed from the perspective of the xz plane. **b)** SEM picture of the type A prototype. **c)** The Poisson's ratio for compression along the z-axis calculated for the topmost row of unit-cells for both types of the considered 3D systems. The geometric parameters corresponding to the predeformed type A structure were the following: $\theta_0 = 90°$, $\theta_1 = 70°$, $a_1 \approx 33.2\,\mu$m, $a_2 \approx 33.8\,\mu$m, $b \approx 22.4\,\mu$m, $d_1 \approx 7.0\,\mu$m, $d_2 \approx 4.0\,\mu$m, $d_3 \approx 6.6\,\mu$m, $d_4 \approx 4.1\,\mu$m, $l \approx 88.7\,\mu$m and $h \approx 16.4\,\mu$m. On the other hand, for the type B system, these parameters were set to be as follows: $\theta_0 = 100°$, $\theta_1 = 70°$, $a_1 \approx 73.5\,\mu$m, $a_2 \approx 74.5\,\mu$m, $b \approx 44.4\,\mu$m, $d_1 \approx 2.6\,\mu$m, $d_2 \approx 9.2\,\mu$m, $d_3 \approx 14.5\,\mu$m, $d_4 \approx 12.5\,\mu$m, $l \approx 180\,\mu$m and $h \approx 33\,\mu$m . For pictures on panels (a-b), the blue dashed line indicates the dimensions of the undeformed structure in the xz plane.

a more challenging manufacturing process.

2.3 Shape morphing

In addition to the possibility of controlling the magnitude of the Poisson's ratio exhibited by the analyzed system, another very interesting direction of studies corresponds to the ability of the hierarchical structure to change its shape during the deformation process. In fact, in **Fig. 2**, it was shown that depending on the thicknesses of hinges, the entire unit-cell may assume different shapes. Thus, in theory, if one would construct the composite mechanical metamaterial consisting of unit-cells associated with multiple different sets of geometric parameters, then it would be possible to obtain the hierarchical structure with the local change in shape as well as mechanical properties. To demonstrate it, one such example is considered in this study.

As shown in **Fig. 4**, the hierarchical mechanical metamaterial composed of $4 \times 3 \times 4$ case 1 unit-cells and $4 \times 3 \times 2$ case 2 unit-cells (see **Fig.4(a-b)**) is considered in order to analyse its ability to change shape in a controllable manner. More specifically, the objective is to change the shape of the initial cuboid-like structure to match the shape of the reference object in the form of the mug presented in **Fig. 4(d)** (see

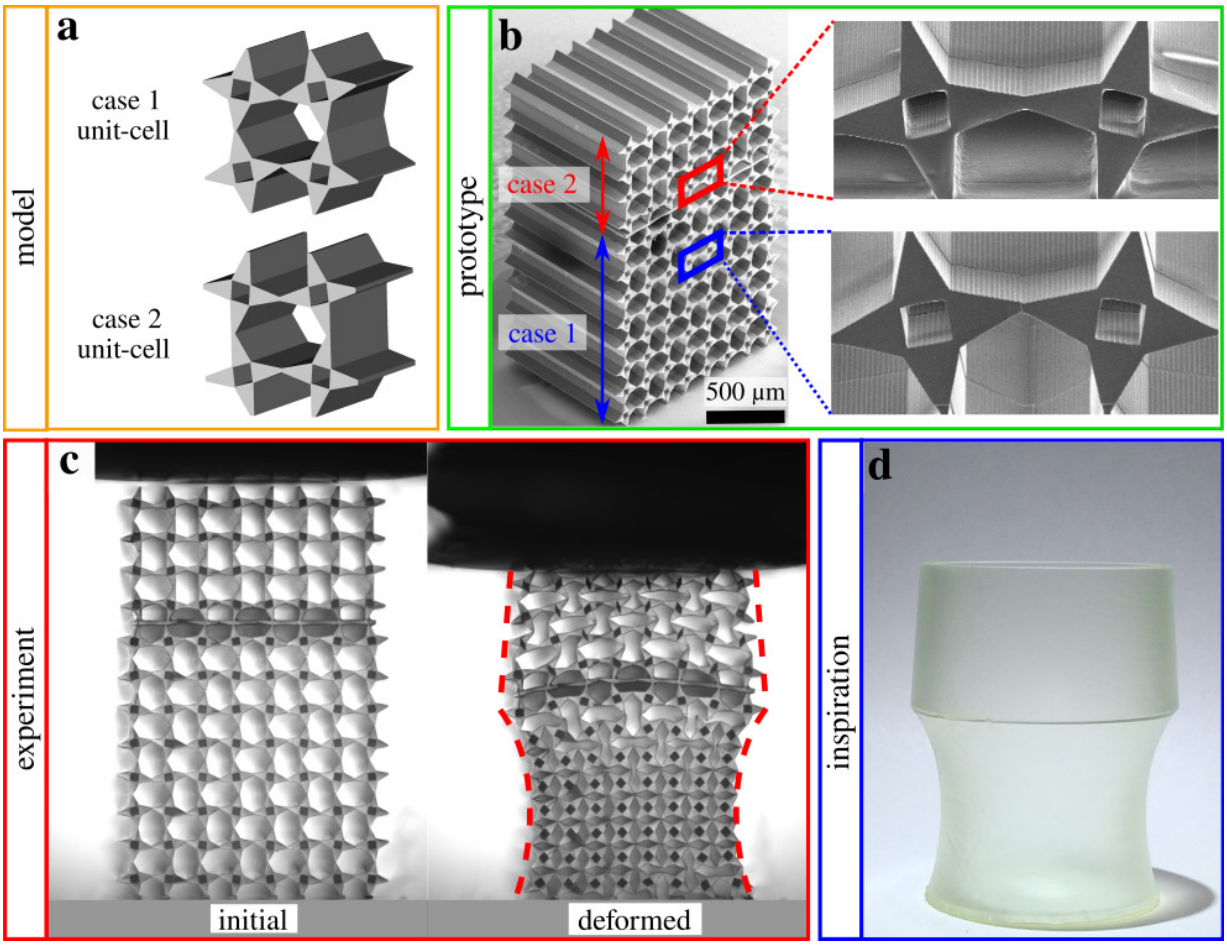

Figure 4: Shape morphing of the considered hierarchical mechanical metamaterials aimed towards the possibility of replicating the shape of the reference object. **a)** A graphical representation of unit-cells corresponding to case 1 and case 2 that were used in the design of the structure that is analyzed from the point of view of its ability to change shape in a predefined manner. **b)** Picture of the prototype used in the experiment together with the zoomed-in images of types of structures used in the design of the resultant composite material. **c)** The experiment corresponding to the compression of the considered structure that results in the change in its shape. **d)** The real-life mug used as an inspiration for the shape that the analyzed hierarchical system is supposed to assume upon being deformed.

Supplementary Video 5). According to **Fig. 4(c)**, upon compressing the system, its shape changes drastically with the bottom part composed of case 1 cells shrinking significantly in the lateral dimension. This effect originates from the strong auxetic behavior that is characteristic for case 1 unit-cells (see **Fig.2**). On the other hand, even though the top part of the hierarchical system consisting of case 2 unit-cells also shrinks in the lateral dimension, the extent of such shrinkage is much smaller than is observed for the bottom part of the structure. This change in the behavior can be explained by the much smaller extent of the auxeticity corresponding to the unit-cell referred to as case 2. Thus, overall, **Fig. 4(c-d)** shows that by designing the hierarchical structure considered in this work in the specific composite-like manner, the entire system may undergo a shape morphing into a much more complex configuration. Of course, the considered example is relatively simple but it proves that in general, one can use the concept presented in this work in order to observe very complex shape morphing at the micro-scale. At this point, it is also worth to mention that in the case of the specific design considered in this study, the two types of materials were connected by means of an additional thin plate that was constraining topmost case 1 cells and bottommost case 2 cells. As a result, at the end of the deformation process, one can observe a big difference in the horizontal dimension of the middle and the top part of the case 1 structure. In fact, the same effect could be achieved if one was to replace the plate with one additional row of very stiff unit-cells. Of course, without the additional plate, a similar behavior is still expected to be observed due to a large difference in the Poisson's ratio between the two types of structures. Nevertheless, such

system would be more difficult to manufacture and the change in the horizontal dimension of the middle and top part of the case 1 structure would be expected to be smaller.

The results reported in this study clearly show that the considered hierarchical structure can be constructed at the microscale and that its mechanical properties with the emphasis on the exhibited Poisson's ratio may be controlled and significantly modified depending on the small change in the design parameters. It should be also mentioned that in theory, such control over the extent of the exhibited auxeticity could be achieved in an active manner, i.e. without the need of reconstructing the system. In this regard, it should be noted that in the case of this work, the behavior of the hierarchical structures is considered for the quasi-static compression where the moment of inertia of structural elements does not affect the results. However, for fast deformations, the rate at which the structure is being compressed could become another factor that allows to determine whether both hierarchical levels are deforming to a large extent. Of course, for this effect to be observed, hinges would have to be appropriately thin with respect to the considered deformation rates (see **Supplementary Information**). In addition, the active control over the behavior of the structure could be achieved through the use of external stimulus such as a change in temperature assuming the use of materials corresponding to the high thermal expansion coefficient while designing the hinges.

In view of all of the above, it is important to emphasize the fact that the results of this work may prove to be of great significance in the case of numerous applications. First of all, the ability of the considered hierarchical mechanical metamaterial to exhibit a very broad range of the auxetic behavior may lead to the design of highly efficient protective equipment (especially for the macroscopic version of the considered concept). In fact, as shown in the **Supplementary Information**, depending on the type of the analyzed structure, the specific energy absorption of the system may be significantly adjusted with its estimated values ranging between 133.2 J kg^{-1} and 386.6 J kg^{-1}. Hence, the considered tunable properties are also interesting from the perspective of impact absorption devices. In addition, the concept proposed in this work may be used in the design of tunable vibration dampers utilizing local vibration isolation. This stems from the fact that as shown in the **Supplementary Information**, the stiffness of the system can be adjusted depending amongst others on the thickness of its hinges. This in turn is a commonly desired feature related to vibration damping devices. In addition, the considered concept is particularly interesting since the model proposed in this work is not solely limited to two-dimensional structures where the devices making use of the provided results could only exhibit their properties in a single plane. Furthermore, the ability of the analyzed system to exhibit shape morphing may significantly increase the efficiency of multiple medical devices including stents by providing localized support for specific parts of the blood vessel that need additional reinforcement. Finally, the shape morphing ability could also be utilized in the design of flexible electronics and equipment used on spacecraft that could adjust its shape upon being deployed from the initially confined configuration that does not waste space onboard prior to being used.

3 Conclusion

In this work, it is shown that the novel microscopic hierarchical mechanical metamaterial can exhibit a wide range of the auxetic behavior depending solely on the change in the thickness of hinges connecting its structural elements. It is also demonstrated that the considered concept can be observed both for the quasi-2D and 3D version of the structure which enables the system to exhibit a desired mechanical response upon being subjected to a deformation induced from different directions. Furthermore, it is presented that the considered structure can exhibit shape morphing allowing it to match the shape of the reference object upon being deformed. It should be noted that different aspects of these results offer a new perspective with regards to the capabilities of hierarchical mechanical metamaterials and are likely to pave the way for other researchers to design similar microscopic functional materials that will further enhance their properties. Finally, it should be emphasized that the presented results may be utilized in

numerous applications. More specifically, the ability of considered hierarchical metamaterials to exhibit a broad range of the auxetic behavior could be important in the design of the protective equipment and vibration dampers. On the other hand, the ability of the considered structure to exhibit shape morphing is very promising for example from the point of view of medical devices capable of locally adjusting their properties as well as flexible electronics.

4 Methods

4.1 Fabrication

The micro-scale samples investigated in this work were fabricated by polymerizing individual unit-cells assuming a small overlap between the adjacent cells. Such overlap was introduced to ensure that the adjacent unit-cells would be connected to each other to form larger composites analyzed in this study. To this aim, the commercial 3D printer (Photonic Professional GT+, Nanoscribe GmbH) operating based on the two-photon lithography method was used. The photoresin selected to produce the analyzed mechanical metamaterials was the commercial negative tone IP-S resin (Nanoscribe GmbH) that is customized to work well with the Nanoscribe 3D printer. Furthermore, the slicing and hatching distances associated with the samples were set to be equal to 1 μm and 0.5 μm respectively. A drop of IP-S resin was deposited on a ITO-coated soda lime glass substrate with dimensions $25 \times 25 \times 0.7$ mm^3 and photopolymerized with a femtosecond laser operating at $\lambda = 780$ nm and a 25X-objective. After printing, the sample was developed for 25 min in Propylene glycol methyl ether acetate (PGMEA) solution to remove the unexposed photoresist and rinsed for 3 min in Isopropyl alcohol (IPA) to clear the developer. A Laser Power of 90 and a Galvanometric scan speed of 100 mm s^{-1} were used for the whole fabrication process. Finally, to improve the adhesion properties of IP-S resin and so to ensure a better connection of the printed sample with the substrate, ITO-coated substrates are pre-treated with oxygen plasma (Corial 200R, RIE etch system) for 5 min. As a result, the bottom part of the samples was constrained from the movement during the deformation process.

4.2 Testing

To test the mechanical properties of the analyzed samples, they were uniaxially compressed at the constant rate of 1 μm/s. The intendter used to induce the compression had a circular polished surface corresponding to the diameter approximately equal to 3 mm. Each sample was placed on top of the leveling table in order to ensure its correct orientation during the experiment. In addition, to ensure the better stabilization, the entire set-up was also placed on top of the optical table. To record the deformation process, an optical camera equipped with a lense corresponding to the 20x and 10x magnification factor was used. It is also worth to mention that prior to the testing, in order to have high-resolution pictures showing the structural details of the printed samples, the SEM microscope was used (Apreo S - Thermofisher). Finally, it should be emphasized that the experiments were continued until the point when hinges connecting adjacent structural elements were breaking at large strains. In addition, to assess whether a given breaking hinge was significantly affecting the deformation pattern, the force vs displacement relationship was analyzed throughout the experiment (see **Supplementary Information**). It should be also emphasized that if one was to construct the system with more durable hinges, then considered structures could be deformed to an even larger extent than is the case in this study. Furthermore, it should be mentioned that the experimental data presented in Fig. 2 were obtained based on pictures taken during the experiment by means of the optical camera. To this aim, positions of characteristic vertices (e.g. edges of hinges connecting level 0 and level 1 blocks) were extracted from respective pictures and utilized to calculate the desired geometric parameters by means of standard mathematical operations.

4.3 FEA simulations

To ensure the validity of the experimental results, the mechanical behavior of the analyzed hierarchical metamaterials was analyzed by means of the FEA simulations. To do this, COMSOL Multiphysics software was used (see **Supplementary Information** to find governing equations corresponding to the considered type of FEM simulations). Since the behavior of the structure was investigated solely from the point of view of its deformation, only the Structural Mechanics module was implemented. In addition, to minimize the computation time, the geometries of the quasi-2D experimental prototypes analyzed in this study were converted into regular 2D structures. Furthermore, to replicate the behavior of the experimental prototypes, the surfaces at the bottom of the structure were fixed in space. Thus, as the samples were compressed, the bottom part of the system could not move. Such deformation process associated with the uniaxial compression of the system was induced through the use of the external indenter pushing the topmost part of the structure downwards. Finally, it should be mentioned that the material corresponding to the analyzed samples was assumed to be isotropic and its properties were set to be the following: $\nu = 0.4$, $E = 4$ GPa. It should be noted that for the considered structures, the selection of the model of elasticity does not significantly affect the mechanical behavior of the system since it depends primarily on its design (see **Supplementary Information**). Furthermore, it should be emphasized that while the considered geometry is nonlinear, the conducted FEM simulations were linear. This stems from the fact that the considered structures are deforming primarily through hinging of structural elements that are retaining their shape throughout the deformation. Thus, the plasticity of a material is not significant from the point of view of the deformation of considered structures and internal stresses are relatively small in comparison to the Young's modulus of the polymer. At this point, even though the following does not belong to the scope of this work, it should be also mentioned that deriving dynamics-related properties would be very difficult in the general case for this work since they would always depend on the material's non-linear properties [69].

Supporting Information
Supporting Information is available from the Wiley Online Library or from the corresponding author.

Acknowledgements
This work was partly supported by the french RENATECH network and its FEMTO-ST technological facility.
K.K.D. acknowledges the support of the Polish National Science Centre (NCN) in the form of the grant awarded as a part of the SONATINA 5 program, project No. 2021/40/C/ST5/00007 under the name "Programmable magneto-mechanical metamaterials guided by the magnetic field".
K.K.D. acknowledges the financial support from the program of the Polish Ministry of Science and Higher Education under the name "Regional Initiative of Excellence" in 2019-2022, project no. 003/RID/2018/19, funding amount 11 936 596.10 PLN.

References

[1] R. M. Neville, F. Scarpa, A. Pirrera, *Sci. Rep.* **2016**, *6,* 31067.

[2] B. Florijn, C. Coulais, M. van Hecke, *Phys. Rev. Lett.* **2014**, *113,* 175503.

[3] C. Coulais, E. Teomy, K. de Reus, Y. Shokef, M. van Hecke, *Nature* **2016**, *535,* 529.

[4] C. Coulais, A. Sabbadini, F. Vink, M. van Hecke, *Nature* **2018**, *561,* 512.

[5] F. Wenz, I. Schmidt, A. Leichner, T. Lichti, S. Baumann, H. Andrae, C. Eberl, *Adv. Mater.* **2021**, *33,* 2008617.

[6] Y. Zhu, M. Birla, K. R. Oldham, E. T. Filipov, *Adv. Funct. Mater.* **2020**, *30,* 2003741.

[7] A. S. Gladman, E. A. Matsumoto, R. G. Nuzzo, L. Mahadevan, J. A. Lewis, *Nat. Mater.* **2016**, *15,* 413.

[8] M. J. Mirzaali, S. Janbaz, M. Strano, L. Vergani, A. A. Zadpoor, *Sci. Rep.* **2018**, *8,* 965.

[9] R. Fleury, D. L. Sounas, C. F. Fleck, M. R. Haberman, A. Alú, *Science* **2014**, *343,* 516.

[10] R. Fleury, D. L. Sounas, A. Alú, *Nat. Commun.* **2015**, *6,* 5905.

[11] H. Liu, Q. Zhang, K. Zhang, G. Hu, H. Duan, *Adv. Sci.* **2019**, *6,* 1900401.

[12] G. W. Miltion, *The Theory of Composites*, Cambridge University Press, Cambridge, UK, **2002**.

[13] G. W. Milton, *J. Mech. Phys.* **2013**, *61,* 1543.

[14] J. A. Jackson, M. C. Messner, N. A. Dudukovic, W. L. Smith, L. Bekker, B. Moran, A. M. Golobic, A. J. Pascall, E. B. Duoss, K. J. Loh, C. M. Spadaccini, *Sci. Adv.* **2018**, *4,* eaau6419.

[15] J. Qi, Z. Chen, P. Jiang, W. Hu, Y. Wang, Z. Zhao, X. Cao, S. Zhang, R. Tao, Y. Li, D. Fang, *Adv. Sci.* **2021**, 2102662.

[16] R. Galea, K. K. Dudek, P.-S. Farrugia, L. Z. Mangion, J. N. Grima, R. Gatt, *Compos. Struct.* **2022**, *280,* 114921.

[17] L. M. Korpas, R. Yin, H. Yasuda, J. R. Raney, *ACS Appl. Mater. Interfaces* **2021**, *13,* 31163.

[18] X. Xin, L. Liu, Y. Liu, J. Leng, *Adv. Funct. Mater.* **2020**, *30,* 2004226.

[19] A. Rafsanjani, K. Bertoldi, A. R. Studart, *Sci. Robot.* **2019**, *4,* eaav7874.

[20] P. Cai, C. Wang, H. Gao, X. Chen, *Adv. Mater.* **2021**, *33,* 2007977.

[21] J. T. B. Overvelde, J. C. Weaver, C. Hoberman, K. Bertoldi, *Nature* **2017**, *541,* 347.

[22] C. Song, B. Zou, Z. Cui, Z. Liang, J. Ju, *Adv. Funct. Mater.* **2021**, *31,* 2101395.

[23] S. Li, G. Librandi, Y. Yao, A. J. Richard, A. Schneider-Yamamura, J. Aizenberg, K. Bertoldi, *Adv. Mater.* **2021**, *33,* 2105024.

[24] A. Russo, B. Y. Ahn, J. J. Adams, E. B. Duoss, J. T. Bernhard, J. A. Lewis, *Adv. Mater.* **2011**, *23,* 3426.

[25] X. Xu, B. Peng, D. Li, J. Zhang, L. M. Wong, Q. Zhang, S. Wang, Q. Xiong, *Nano Lett.* **2011**, *11,* 3232.

[26] H. M. A. Kolken, S. Janbaz, S. M. A. Leeflang, K. Lietaert, H. H. Weinans, A. A. Zadpoor, *Mater. Horiz.* **2018**, *5,* 28.

[27] T. van Manen, S. Janbaz, K. M. B. Jansen, A. A. Zadpoor, *Commun. Mater.* **2021**, *2,* 56.

[28] K. E. Evans, M. A. Nkansah, I. J. Hutchinson, S. C. Rogers, *Nature* **1991**, *353,* 124.

[29] J. N. Grima, R. Caruana-Gauci, *Nat. Mater.* **2012**, *11,* 565.

[30] K. Bertoldi, V. Vitelli, J. Christensen, M. van Hecke, *Nat. Rev. Mater.* **2017**, *2,* 17066.

[31] M. Kadic, G. M. Milton, M. van Hecke, M. Wegener, *Nat. Rev. Phys.* **2019**, *1,* 198.

[32] C. Kern, G. W. Milton, M. Kadic, M. Wegener, *New J. Phys.* **2018**, *20,* 083034.

[33] K. W. Wojciechowski, *Phys. Lett. A* **1989**, *137,* 60.

[34] R. Lakes, *Science* **1987**, *235,* 1038.

[35] K. E. Evans, A. Alderson, *Adv. Mater.* **2000**, *12,* 617.

[36] N. Novak, L. Biasetto, P. Rebesan, F. Zanini, S. Carmignato, L. Krstulović-Opara, M. Vesenjak, Z. Ren, *Addit. Manuf.* **2021**, *45,* 102022.

[37] T.-C. Lim, *Compos. Struct.* **2019**, *209,* 34.

[38] L. Mizzi, K. M. Azzopardi, D. Attard, J. N. Grima, R. Gatt, *Phys. Status Solidi RRL* **2015**, *9,* 425.

[39] J. N. Grima-Cornish, R. Cauchi, D. Attard, R. Gatt, J. N. Grima, *Phys. Status Solidi B* **2020**, *257,* 1900707.

[40] P.-S. Farrugia, R. Gatt, J. N. Grima-Cornish, J. N. Grima, *Phys. Status Solidi B* **2020**, *257,* 1900507.

[41] T. A. M. Hewage, K. L. Alderson, A. Alderson, F. Scarpa, *Adv. Mater.* **2016**, *28,* 10323.

[42] Z. G. Nicolaou, A. E. Motter, *Nat. Mater.* **2012**, *11,* 608.

[43] R. H. Baughman, S. Stafstrom, C. Cui, S. O. Dantas, *Science* **1998**, *279,* 1522.

[44] R. Lakes, *Nature* **1993**, *361,* 511.

[45] R. Gatt, L. Mizzi, J. I. Azzopardi, K. M. Azzopardi, D. Attard, A. Casha, J. Briffa, J. N. Grima, *Sci. Rep.* **2015**, *5,* 8395.

[46] Y. Cho, J.-H. Shin, A. Costa, V. K. T. A. Kim, J. Li, S. Y. Lee, S. Yang, H. N. Han, I.-S. Choi, D. J. Srolovitz, *Proc. Natl. Acad. Sci.* **2014**, *111,* 17390.

[47] Y. Tang, G. Lin, L. Han, S. Qiu, S. Yang, J. Yin, *Adv. Mater.* **2015**, *27,* 7181.

[48] K. K. Dudek, R. Gatt, M. R. Dudek, J. N. Grima, *Materials* **2021**, *14,* 758.

[49] J. Cai, A. Akbarzadeh, *Mater. Des.* **2021**, *206,* 109811.

[50] X. Li, R. Fan, Z. Fan, Y. Lu, *Int. J. Solids Struct.* **2021**, *216,* 145.

[51] L. Mizzi, A. Spaggiari, *Smart Mater. Struct.* **2020**, *29,* 105036.

[52] N. An, A. G. Domel, J. Zhou, A. Rafsanjani, K. Bertoldi, *Adv. Funct. Mater.* **2020**, *30,* 1906711.

[53] K. Billon, I. Zampetakis, F. Scarpa, M. Ouisse, E. Sadoulet-Reboul, M. Collet, A. Perriman, A. Hetherington, *Compos. Struct.* **2017**, *160,* 1042.

[54] Y. Tang, J. Yin, *Extreme Mech. Lett.* **2017**, *12,* 77.

[55] R. Oftadeh, B. Haghpanah, D. Vella, A. Boudaoud, A. Vaziri, *Phys. Rev. Lett.* **2014**, *113,* 104301.

[56] D. Mousanezhad, S. Babaee, H. Ebrahimi, R. Ghosh, A. S. Hamouda, K. Bertoldi, A. Vaziri, *Sci. Rep.* **2016**, *5,* 18306.

[57] Y. Chen, T. Li, Z. Jia, F. Scarpa, C.-W. Yao, L. Wang, *Mater. Des.* **2018**, *137,* 226.

[58] D. Zhang, Q. Fei, J. Liu, D. Jiang, Y. Li, *Thin-Walled Struct.* **2020**, *146,* 106436.

[59] L. R. Meza, A. J. Zelhofer, N. Clarke, A. J. Mateos, D. M. Kochmann, J. R. Greer, *Proc. Natl. Acad. Sci. U. S. A.* **2015**, *112,* 11502.

[60] J. Shi, A. H. Akbarzadeh, *Int. J. Eng. Sci.* **2020**, *149,* 103247.

[61] X. Zhang, Y. Zheng, X. Liu, W. Lu, J. Dai, D. Y. Lei, D. R. MacFarlane, *Adv. Mater.* **2015**, *27,* 1090.

[62] K. K. Dudek, D. Attard, R. Caruana-Gauci, K. W. Wojciechowski, J. N. Grima, *Smart Mater. Struct.* **2016**, *25,* 025009.

[63] J. N. Grima, K. E. Evans, *J. Mater. Sci. Lett.* **2000**, *19,* 1563.

[64] J. N. Grima, R. Gatt, A. Alderson, K. E. Evans, *J. Phys. Soc. Japan* **2005**, *74,* 2866.

[65] J. N. Grima, R. Gatt, B. Ellul, E. Chetcuti, *J. Non. Cryst. Solids* **2010**, *356,* 1980.

[66] J. N. Grima, K. E. Evans, *J. Mater. Sci.* **2006**, *41,* 3193.

[67] X.-Q. Zhou, L. Zhang, L. Yang, *Chin. Phys. B* **2017**, *26,* 126201.

[68] J. N. Grima, E. Chetcuti, E. Manicaro, D. Attard, M. Camilleri, R. Gatt, K. E. Evans, *Proc. R. Soc. A.* **2011**, *468,* 810.

[69] W. J. Parnell, A. N. Norris, T. Shearer, *Appl. Phys. Lett.* **2012**, *100,* 171907.